The associated powers are calculated according to (1.7.3.8), which leads to

$$P(L) = m(n/2)(\varepsilon_o/\mu_o)^{1/2}|E_o|^2\pi w_o^2 \qquad (1.7.3.38)$$

where $m = 1$ for a flat distribution and $m = 1/2$ for a Gaussian profile.

The nonlinear interaction is characterized by the conversion efficiency, which is defined as the ratio of the generated power to the power of one or several incident beams, according to the different kinds of interactions.

For pulsed beams, it is necessary to consider the temporal shape, usually Gaussian:

$$P(t) = P_c \exp(-2t^2/\tau^2) \qquad (1.7.3.39)$$

where P_c is the peak power and τ the half $(1/e^2)$ width.

For a repetition rate f (s^{-1}), the average power $\tilde{P}$ is then given by

$$\tilde{P} = P_c\tau f(\pi/2)^{1/2} = \tilde{E}f \qquad (1.7.3.40)$$

where $\tilde{E}$ is the energy per Gaussian pulse.

When the pulse shape is not well defined, it is suitable to consider the energies per pulse of the incident and generated waves for the definition of the conversion efficiency.

The interactions studied here are sum-frequency generation (SFG), including second harmonic generation (SHG: $\omega + \omega = 2\omega$), cascading third harmonic generation (THG: $\omega + 2\omega = 3\omega$) and direct third harmonic generation (THG: $\omega + \omega + \omega = 3\omega$). The difference-frequency generation (DFG) is also considered, including optical parametric amplification (OPA) and oscillation (OPO).

We choose to analyse in detail the different parameters relative to conversion efficiency (figure of merit, acceptance bandwidths, walk-off effect *etc.*) for SHG, which is the prototypical second-order nonlinear interaction. This discussion will be valid for the other nonlinear processes of frequency generation which will be considered later.

1.7.3.3.2. *Second harmonic generation (SHG)*

According to Table 1.7.3.1, there are two types of phase matching for SHG: type I and type II (equivalent to type III).

The fundamental waves at ω define the pump. Two situations are classically distinguished: the undepleted pump approximation, when the power conversion efficiency is sufficiently low to consider the fundamental power to be undepleted, and the depleted case for higher efficiency. There are different ways to realize SHG, as shown in Fig. 1.7.3.6: the simplest one is non-resonant SHG, outside the laser cavity; other ways are external or internal resonant cavity SHG, which allow an enhancement of the single-pass efficiency conversion.

1.7.3.3.2.1. *Non-resonant SHG with undepleted pump in the parallel-beam limit with a Gaussian transverse profile*

We first consider the case where the crystal length is short enough to be located in the near-field region of the laser beam where the parallel-beam limit is a good approximation. We make another simplification by considering a propagation along a principal axis of the index surface: then the walk-off angle of each interacting wave is nil so that the three waves have the same coordinate system (X, Y, Z).

The integration of equations (1.7.3.22) over the crystal length Z in the undepleted pump approximation, *i.e.* $\partial E_1^\omega(X, Y, Z)/\partial Z = \partial E_2^\omega(X, Y, Z)/\partial Z = 0$, with $E_3^{2\omega}(X, Y, 0) = 0$, leads to

$$|E_3^{2\omega}(X, Y, L)|^2 = \{K_3^{2\omega}[\varepsilon_o\chi_{\rm eff}^{(2)}]\}^2|E_1^\omega(X, Y, 0)E_2^\omega(X, Y, 0)|^2 \times L^2\sin c^2[(\Delta k \cdot L)/2]. \qquad (1.7.3.41)$$

(1.7.3.41) implies a Gaussian transversal profile for $|E_3^{2\omega}(X, Y, L)|$ if $|E_1^\omega(X, Y, 0)|$ and $|E_2^\omega(X, Y, 0)|$ are Gaussian. The three beam radii are related by $(1/w_{o3}^2) = (1/w_{o1}^2) + (1/w_{o2}^2)$, so if we assume that the two fundamental beams have the same radius w_o^ω, which is not an approximation for type I, then $w_o^{2\omega} = [w_o^\omega/(2^{1/2})]$. Two incident beams with a flat distribution of radius w_o^ω lead to the generation of a flat harmonic beam with the same radius $w_o^{2\omega} = w_o^\omega$.

The integration of (1.7.3.41) according to (1.7.3.36)–(1.7.3.38) for a Gaussian profile gives in the SI system

$$P^{2\omega}(L) = BP_1^\omega(0)P_2^\omega(0)\frac{L^2}{w_o^2}\sin c^2\left(\frac{\Delta k \cdot L}{2}\right)$$
$$B = \frac{32\pi}{\varepsilon_o c}\frac{2N-1}{N}\frac{d_{\rm eff}^2}{\lambda_\omega^2}\frac{T_3^{2\omega}T_1^\omega T_2^\omega}{n_3^{2\omega}n_1^\omega n_2^\omega}, \quad ({\rm W}^{-1}) \qquad (1.7.3.42)$$

where $c = 3 \times 10^8$ m s^{-1}, $\varepsilon_o = 8.854 \times 10^{-12}$ A s V^{-1} m^{-1} and so $(32\pi/\varepsilon_o c) = 37.85 \times 10^3$ V A^{-1}. L (m) is the crystal length in the direction of propagation. $\Delta k = k_3^{2\omega} - k_1^\omega - k_2^\omega$ is the phase mismatch. $n_3^{2\omega}$, n_1^ω and n_2^ω are the refractive indices at the harmonic and fundamental wavelengths $\lambda_{2\omega}$ and λ_ω (µm): for the phase-matching case, $\Delta k = 0$, $n_3^{2\omega} = n^-(2\omega)$, $n_1^\omega = n_2^\omega = n^+(\omega)$ for type I (the two incident fundamental beams have the same polarization contained in Π^+, with the harmonic polarization contained in Π^-) and $n_1^\omega = n^+(\omega) \neq n_2^\omega = n^-(\omega)$ for type II (the two solicited eigen modes at the fundamental wavelength are in Π^+ and Π^-, with the harmonic polarization contained in Π^-). $T_3^{2\omega}$, T_1^ω and T_2^ω are the transmission coefficients given by $T_i = 4n_i/(n_i + 1)^2$. $d_{\rm eff}$ (pm V^{-1}) $= (1/2)\chi_{\rm eff} = (1/2)[F^{(2)} \cdot \chi^{(2)}]$ is the effective coefficient given by (1.7.3.30) and (1.7.3.31). $P_1^\omega(0)$ and $P_2^\omega(0)$ are the two incident fundamental powers, which are not necessarily equal for type II; for type I we have obviously $P_1^\omega(0) = P_2^\omega(0) = (P_{\rm tot}^\omega/2)$. N is the number of independently oscillating modes at the fundamental wavelength: every longitudinal mode at the harmonic pulsation can be generated by many combinations of two fundamental modes; the $(2N-1)/N$ factor takes into account the fluctuations between these longitudinal modes (Bloembergen, 1963).

The powers in (1.7.3.42) are instantaneous powers $P(t)$.

The second harmonic (SH) conversion efficiency, $\eta_{\rm SHG}$, is usually defined as the ratio of peak powers $P_c^{2\omega}(L)/P_{c,{\rm tot}}^\omega(0)$, or as the ratio of the pulse total energy $\tilde{E}^{2\omega}(L)/\tilde{E}_{\rm tot}^\omega(0)$. For Gaussian temporal profiles, the SH $(1/e^2)$ pulse duration $\tau_{2\omega}$ is equal to $\tau_\omega/(2^{1/2})$, because $P_{2\omega}$ is proportional to P_ω^2, and so, according to (1.7.3.40), the pulse average energy conversion efficiency is $1/(2^{1/2})$ smaller than the peak power conversion efficiency given by (1.7.3.42). Note that the pulse total energy conversion efficiency is equivalent to the average power conversion efficiency $\tilde{P}^{2\omega}(L)/\tilde{P}_{\rm tot}^\omega(0)$, with $\tilde{P} = \tilde{E} \cdot f$ where f is the repetition rate.

Formula (1.7.3.42) shows the importance of the contribution of the linear optical properties to the nonlinear process. Indeed, the field tensor $F^{(2)}$, the transmission coefficients T_i and the phase mismatch Δk only depend on the refractive indices in the direction of propagation considered.

(i) *Figure of merit*.

The contribution of $F^{(2)}$ was discussed previously, where it was shown that the field tensor is nil in particular directions of propagation or everywhere for particular crystal classes and configurations of polarization (even if the nonlinearity $\chi^{(2)}$ is high).

The field tensor $F^{(2)}$ of SHG can be written with the contracted notation of $d^{(2)}$; according to Table 1.7.3.1 and to the contraction

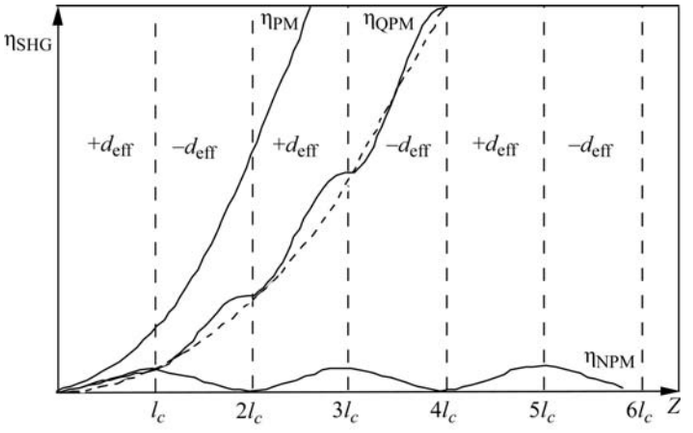

Fig. 1.7.3.7. Spatial growth evolution of second harmonic conversion efficiency, η_{SHG}, for non phase matching (NPM), $\Delta k \neq 0$, and phase matching (PM), $\Delta k = 0$, in a 'continuous' crystal, and for quasi phase matching (QPM) in a periodic structure. The dashed curve corresponds to $(4/\pi^2)\eta_{PM}(Z)$ where η_{PM} is the conversion efficiency of the phase-matched SHG. $l_c = \pi/\Delta k$ is the coherence length.

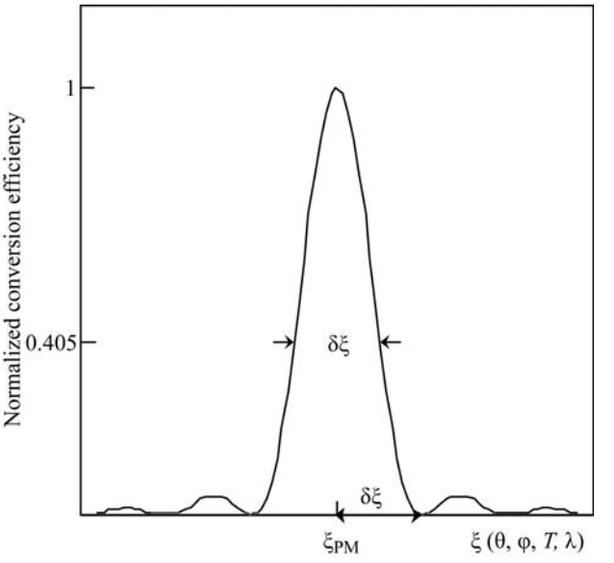

Fig. 1.7.3.8. Conversion efficiency evolution as a function of ξ for a given crystal length. ξ denotes the angle (θ or φ), the temperature (T) or the wavelength (λ). ξ_{PM} represents the parameter allowing phase matching.

conventions given in Section 1.7.2.2, the contracted field-tensor components for the phase-matched SHG are

$$\begin{aligned}
F_{i1} &= \mathbf{e}_i^-(2\omega)[\mathbf{e}_x^+(\omega)]^2 \\
F_{i2} &= \mathbf{e}_i^-(2\omega)[\mathbf{e}_y^+(\omega)]^2 \\
F_{i3} &= \mathbf{e}_i^-(2\omega)[\mathbf{e}_z^+(\omega)]^2 \\
F_{i4} &= 2\mathbf{e}_i^-(2\omega)\mathbf{e}_y^+(\omega)\mathbf{e}_z^+(\omega) \\
F_{i5} &= 2\mathbf{e}_i^-(2\omega)\mathbf{e}_x^+(\omega)\mathbf{e}_z^+(\omega) \\
F_{i6} &= 2\mathbf{e}_i^-(2\omega)\mathbf{e}_x^+(\omega)\mathbf{e}_y^+(\omega)
\end{aligned}$$

for type I and

$$\begin{aligned}
F_{i1} &= \mathbf{e}_i^-(2\omega)\mathbf{e}_x^+(\omega)\mathbf{e}_x^-(\omega) \\
F_{i2} &= \mathbf{e}_i^-(2\omega)\mathbf{e}_y^+(\omega)\mathbf{e}_y^-(\omega) \\
F_{i3} &= \mathbf{e}_i^-(2\omega)\mathbf{e}_z^+(\omega)\mathbf{e}_z^-(\omega) \\
F_{i4} &= \mathbf{e}_i^-(2\omega)[\mathbf{e}_y^+(\omega)\mathbf{e}_z^-(\omega) + \mathbf{e}_y^-(\omega)\mathbf{e}_z^+(\omega)] \\
F_{i5} &= \mathbf{e}_i^-(2\omega)[\mathbf{e}_x^+(\omega)\mathbf{e}_z^-(\omega) + \mathbf{e}_x^-(\omega)\mathbf{e}_z^+(\omega)] \\
F_{i6} &= \mathbf{e}_i^-(2\omega)[\mathbf{e}_x^+(\omega)\mathbf{e}_y^-(\omega) + \mathbf{e}_x^-(\omega)\mathbf{e}_y^+(\omega)]
\end{aligned}$$

for type II, with $i = (1, 2, 3)$ for F_{ij}, corresponding to $i = (x, y, z)$ for $\mathbf{e}_i^-(2\omega)$.

The ratio $d_{eff}^2/n_3^{2\omega}n_1^{\omega}n_2^{\omega}$ in formula (1.7.3.42) is called the figure of merit of the direction considered. The effective coefficient is given in Section 1.7.5 for the main nonlinear crystals and for chosen SHG wavelengths.

(ii) *Effect of the phase mismatch.*

The interference function $\sin c^2(\Delta kL/2)$ is a maximum and equal to unity only for $\Delta k = 0$, which defines the phase-matching condition. Fig. 1.7.3.7 shows the effect of the phase mismatch on the growth of second harmonic conversion efficiency, η_{SHG}, with interaction distance Z.

The conversion efficiency has a Z^2 dependence in the case of phase matching. The harmonic power oscillates around Z^2 for quasi phase matching, but is reduced by a factor of $4/\pi^2$ compared with that of phase-matched interaction (Fejer *et al.*, 1992).

An SHG phase-matching direction $(\theta_{PM}, \varphi_{PM})$ for given fundamental wavelength (λ_{PM}) and type of interaction, I or II, is defined at a given temperature (T_{PM}). It is important to consider the effect of deviation of Δk from 0 due to variations of angles $(\theta_{PM} \pm d\theta, \varphi_{PM} \pm d\varphi)$, of temperature $(T_{PM} \pm dT)$ and of wavelength $(\lambda_{PM} \pm d\lambda)$ on the conversion efficiency. The quantities that characterize these effects are the acceptance bandwidths $\delta\xi$ $(\xi = \theta, \varphi, T, \lambda)$, usually defined as the deviation from the phase-matching value ξ_{PM} leading to a phase-mismatch variation Δk from 0 to $2\pi/L$, where L is the crystal length. Then $\delta\xi$ is also the full width of the peak efficiency curve plotted as a function of ξ at 0.405 of the maximum, as shown in Fig. 1.7.3.8.

Thus $L\delta\xi$ is a characteristic of the phase-matching direction. Small angular, thermal and spectral dispersion of the refractive indices lead to high acceptance bandwidths. The higher $L\delta\xi$, the lower is the decrease of the conversion efficiency corresponding to a given angular shift, to the heating of the crystal due to absorption or external heating, or to the spectral bandwidth of the fundamental beam.

The knowledge of the angular, thermal and spectral dispersion of the refractive indices allows an estimation of $\delta\xi$ by expanding Δk in a Taylor series about ξ_{PM}:

$$\frac{2\pi}{L} = \Delta k = \left.\frac{\partial(\Delta k)}{\partial\xi}\right|_{\xi_{PM}} \delta\xi + \frac{1}{2}\left.\frac{\partial^2(\Delta k)}{\partial\xi^2}\right|_{\xi_{PM}} (\delta\xi)^2 + \ldots . \quad (1.7.3.43)$$

When the second- and higher-order differential terms in (1.7.3.43) are negligible, the phase matching is called critical (CPM), because $L\delta\xi \simeq |2\pi/[\partial(\Delta k)/\partial\xi|_{\xi_{PM}}]|$ is small. For the particular cases where $\partial(\Delta k)/\partial\xi|_{\xi_{PM}} = 0$, $L\delta\xi = \{|4\pi L/[\partial^2(\Delta k)/\partial\xi^2|_{\xi_{PM}}]|\}^{1/2}$ is larger than the CPM acceptance and the phase matching is called non-critical (NCPM) for the parameter ξ considered.

We first consider the case of angular acceptances. In uniaxial crystals, the refractive indices do not vary in φ, leading to an infinite φ angular acceptance bandwidth. $\delta\theta$ is then the only one to consider. For directions of propagation out of the principal plane ($\theta_{PM} \neq \pi/2$), the phase matching is critical. According to the expressions of n_o and $n_e(\theta)$ given in Section 1.7.3.1, we have

(1) for type I in positive crystals, $n_e(\theta, \omega) = n_o(2\omega)$ and

$$L\delta\theta \simeq 2\pi/\{-(\omega/c)n_o^3(2\omega)[n_e^{-2}(\omega) - n_o^{-2}(\omega)]\sin 2\theta_{PM}\}; \quad (1.7.3.44)$$

(2) for type II in positive crystals, $2n_o(2\omega) = n_e(\theta, \omega) + n_o(\omega)$ and

$$L\delta\theta \simeq 2\pi/\{-(\omega/2c)[2n_o(2\omega) - n_o(\omega)]^3 \times [n_e^{-2}(\omega) - n_o^{-2}(\omega)]\sin 2\theta_{\rm PM}\}; \quad (1.7.3.45)$$

(3) for type I in negative crystals, $n_e(\theta, 2\omega) = n_o(\omega)$ and

$$L\delta\theta \simeq 2\pi/\{-(\omega/c)n_o^3(\omega)[n_o^{-2}(2\omega) - n_e^{-2}(2\omega)]\sin 2\theta_{\rm PM}\}; \quad (1.7.3.46)$$

(4) for type II in negative crystals, $2n_e(\theta, 2\omega) = n_e(\theta, \omega) + n_o(\omega)$ and

$$L\delta\theta \simeq \big|2\pi/\{-(\omega/c)n_e^3(\theta, 2\omega)[n_e^{-2}(2\omega) - n_o^{-2}(2\omega)]\sin 2\theta_{\rm PM} + (\omega/2c)n_e^3(\theta, \omega)[n_e^{-2}(\omega) - n_o^{-2}(\omega)]\sin 2\theta_{\rm PM}\}\big|. \quad (1.7.3.47)$$

CPM acceptance bandwidths are small, typically about one mrad cm, as shown in Section 1.7.5 for the classical nonlinear crystals.

When $\theta_{\rm PM} = \pi/2$, $\partial\Delta k/\partial\theta = 0$ and the phase matching is non-critical:

(1) for type I in positive crystals, $n_e(\omega) = n_o(2\omega)$ and

$$L\delta\theta \simeq \big(2\pi L/\{-(\omega/c)n_o^3(2\omega)[n_e^{-2}(\omega) - n_o^{-2}(\omega)]\}\big)^{1/2}; \quad (1.7.3.48)$$

(2) for type II in positive crystals, $2n_o(2\omega) = n_e(\omega) + n_o(\omega)$ and

$$L\delta\theta \simeq \big(2\pi L/\{-(\omega/2c)n_e^3(\omega)[n_e^{-2}(\omega) - n_o^{-2}(\omega)]\}\big)^{1/2}; \quad (1.7.3.49)$$

(3) for type I in negative crystals, $n_o(\omega) = n_e(2\omega)$ and

$$L\delta\theta \simeq \big(2\pi L/\{(\omega/c)n_o^3(\omega)[n_e^{-2}(2\omega) - n_o^{-2}(2\omega)]\}\big)^{1/2}; \quad (1.7.3.50)$$

(4) for type II in negative crystals, $2n_e(2\omega) = n_e(\omega) + n_o(\omega)$ and

$$L\delta\theta \simeq \big(|2\pi L/\{-(\omega/c)n_e^3(2\omega)[n_e^{-2}(2\omega) - n_o^{-2}(2\omega)] + (\omega/2c)n_e^3(\omega)[n_e^{-2}(\omega) - n_o^{-2}(\omega)]\}|\big)^{1/2}. \quad (1.7.3.51)$$

Values of NCPM acceptance bandwidths are given in Section 1.7.5 for the usual crystals. From the previous expressions for CPM and NCPM angular acceptances, it appears that the angular bandwidth is all the smaller since the birefringence is high.

The situation is obviously more complex in the case of biaxial crystals. The φ acceptance bandwidth is not infinite, leading to a smaller anisotropy of the angular acceptance in comparison with uniaxial crystals. The expressions of the θ and φ acceptance bandwidths have the same form as for the uniaxial class only in the principal planes. The phase matching is critical (CPM) for all directions of propagation out of the principal axes x, y and z: in this case, the mismatch Δk is a linear function of small angular deviations from the phase-matching direction as for uniaxial crystals. There exist six possibilities of NCPM for SHG, types I and II along the three principal axes, corresponding to twelve different index conditions (Hobden, 1967):

(1) for positive biaxial crystals

$$\begin{array}{ll} \text{Type I } (x) & n_{2\omega}^y = n_\omega^z \\ \text{Type I } (y) & n_{2\omega}^x = n_\omega^z \\ \text{Type I } (z) & n_{2\omega}^x = n_\omega^y \\ \text{Type II } (x) & n_{2\omega}^y = \tfrac{1}{2}(n_\omega^y + n_\omega^z) \\ \text{Type II } (y) & n_{2\omega}^x = \tfrac{1}{2}(n_\omega^x + n_\omega^z) \\ \text{Type II } (z) & n_{2\omega}^x = \tfrac{1}{2}(n_\omega^x + n_\omega^y); \end{array} \quad (1.7.3.52)$$

(2) for negative biaxial crystals

$$\begin{array}{ll} \text{Type I } (x) & n_{2\omega}^z = n_\omega^y \\ \text{Type I } (y) & n_{2\omega}^z = n_\omega^x \\ \text{Type I } (z) & n_{2\omega}^y = n_\omega^x \\ \text{Type II } (x) & n_{2\omega}^z = \tfrac{1}{2}(n_\omega^y + n_\omega^z) \\ \text{Type II } (y) & n_{2\omega}^z = \tfrac{1}{2}(n_\omega^x + n_\omega^z) \\ \text{Type II } (z) & n_{2\omega}^y = \tfrac{1}{2}(n_\omega^x + n_\omega^y). \end{array}$$

The NCPM angular acceptances along the three principal axes of biaxial crystals can be deduced from the expressions relative to the uniaxial class by the following substitutions:

Along the x axis:

$L\delta\varphi$ (type I > 0) = (1.7.3.50) with $n_o(\omega) \to n_z(\omega)$, $n_e(2\omega) \to n_y(2\omega)$ and $n_o(2\omega) \to n_x(2\omega)$

$L\delta\theta$ (type I > 0) = (1.7.3.48) with $n_o(2\omega) \to n_y(2\omega)$, $n_e(\omega) \to n_z(\omega)$ and $n_o(\omega) \to n_x(\omega)$

$L\delta\varphi$ (type II > 0) = (1.7.3.51) with $n_e \to n_y$ and $n_o \to n_x$

$L\delta\theta$ (type II > 0) = (1.7.3.49) with $n_e(\omega) \to n_z(\omega)$ and $n_o(\omega) \to n_x(\omega)$

$L\delta\varphi$ (type I < 0) = (1.7.3.48) with $n_o(2\omega) \to n_z(2\omega)$, $n_e(\omega) \to n_x(\omega)$ and $n_o(\omega) \to n_y(\omega)$

$L\delta\theta$ (type I < 0) = (1.7.3.50) with $n_o(\omega) \to n_y(\omega)$, $n_e(2\omega) \to n_z(2\omega)$ and $n_o(2\omega) \to n_x(2\omega)$

$L\delta\varphi$ (type II < 0) = (1.7.3.49) with $n_e(\omega) \to n_x(\omega)$ and $n_o(\omega) \to n_y(\omega)$

$L\delta\theta$ (type II < 0) = (1.7.3.51) with $n_e \to n_z$ and $n_o \to n_x$.

Along the y axis:

$L\delta\varphi$ is the same as along the x axis for all interactions

$L\delta\theta$ (type I > 0) = (1.7.3.48) with $n_o(2\omega) \to n_x(2\omega)$, $n_e(\omega) \to n_z(\omega)$ and $n_o(\omega) \to n_y(\omega)$

$L\delta\theta$ (type II > 0) = (1.7.3.49) with $n_e(\omega) \to n_z(\omega)$ and $n_o(\omega) \to n_y(\omega)$

$L\delta\theta$ (type I < 0) = (1.7.3.50) with $n_o(\omega) \to n_x(\omega)$, $n_e(2\omega) \to n_z(2\omega)$ and $n_o(2\omega) \to n_y(2\omega)$

$L\delta\theta$ (type II < 0) = (1.7.3.51) with $n_e \to n_z$ and $n_o \to n_y$.

Along the z axis:

$L\delta\theta_{xz}$ (type I > 0) = (1.7.3.48) with $n_o(2\omega) \to n_y(2\omega)$, $n_e(\omega) \to n_x(\omega)$ and $n_o(\omega) \to n_z(\omega)$

$L\delta\theta_{yz}$ (type I > 0) = (1.7.3.48) with $n_o(2\omega) \to n_x(2\omega)$, $n_e(\omega) \to n_y(\omega)$ and $n_o(\omega) \to n_z(\omega)$

$L\delta\theta_{xz}$ (type II > 0) = (1.7.3.49) with $n_e(\omega) \to n_x(\omega)$ and $n_o(\omega) \to n_z(\omega)$

$L\delta\theta_{yz}$ (type II > 0) = (1.7.3.49) with $n_e(\omega) \to n_y(\omega)$ and $n_o(\omega) \to n_z(\omega)$

$L\delta\theta_{xz}$ (type I < 0) = (1.7.3.50) with $n_o(\omega) \to n_y(\omega)$, $n_e(2\omega) \to n_z(2\omega)$ and $n_o(2\omega) \to n_x(2\omega)$

$L\delta\theta_{yz}$ (type I < 0) = (1.7.3.50) with $n_o(\omega) \to n_x(\omega)$, $n_e(2\omega) \to n_z(2\omega)$ and $n_o(2\omega) \to n_y(2\omega)$

$L\delta\theta_{xz}$ (type II < 0) = (1.7.3.51) with $n_e \rightarrow n_x$ and $n_o \rightarrow n_z$

$L\delta\theta_{yz}$ (type II < 0) = (1.7.3.51) with $n_e \rightarrow n_y$ and $n_o \rightarrow n_z$.

The above formulae are relative to the internal angular acceptance bandwidths. The external acceptance angles are enlarged by a factor of approximately $n(\omega)$ for type I or $[n_1(\omega) + n_2(\omega)]/2$ for type II, due to refraction at the input plane face of the crystal. The angular acceptance is an important issue connected with the accuracy of cutting of the crystal.

Temperature tuning is a possible alternative for achieving NCPM in a few materials. The corresponding temperatures for different interactions are given in Section 1.7.5.

Another alternative is to use a special non-collinear configuration known as one-beam non-critical non-collinear phase matching (OBNC): it is non-critical with respect to the phase-matching angle of one of the input beams (referred to as the non-critical beam). It has been demonstrated that the angular acceptance bandwidth for the non-critical beam is exceptionally large, for example about 50 times that for the critical beam for type-I SHG at 1.338 μm in 3-methyl-4-nitropyridine-*N*-oxide (POM) (Dou *et al.*, 1992).

The typical values of thermal acceptance bandwidth, given in Section 1.7.5, are of the order of 0.5 to 50 K cm. The thermal acceptance is an important issue for the stability of the harmonic power when the absorption at the wavelengths concerned is high or when temperature tuning is used for the achievement of angular NCPM. Typical spectral acceptance bandwidths for SHG are given in Section 1.7.5. The values are of the order of 1 nm cm, which is much larger than the linewidth of a single-frequency laser, except for some diode or for sub-picosecond lasers with a large spectral bandwidth.

Note that a degeneracy of the first-order temperature or spectral derivatives ($\partial\Delta k/\partial T|_{T_{PM}} = 0$ or $\partial\Delta k/\partial\lambda|_{\lambda_{PM}} = 0$) can occur and lead to thermal or spectral NCPM.

Consideration of the phase-matching function $\lambda_{PM} = f(\xi_{PM})$, where $\chi_{PM} = T_{PM}, \theta_{PM}, \varphi_{PM}$ or all other dispersion parameters of the refractive indices, is useful for a direct comparison of the situation of non-criticality of the phase matching relative to λ_{PM} and to the other parameters ξ_{PM}: a nil derivative of λ_{PM} with respect to ξ_{PM}, *i.e.* $d\lambda_{PM}/d\xi_{PM} = 0$ at the point $(\lambda^o_{PM}, \xi^o_{PM})$, means that the phase matching is non-critical with respect to ξ_{PM} and so strongly critical with respect to λ_{PM}, *i.e.* $d\xi_{PM}/d\lambda_{PM} = \infty$ at this point. Then, for example, an angular NCPM direction is a spectral CPM direction and the reverse is also so.

(iii) *Effect of spatial walk-off.*

The interest of the NCPM directions is increased by the fact that the walk-off angle of any wave is nil: the beam overlap is complete inside the nonlinear crystal. Under CPM, the interacting waves propagate with different walk-off angles: the conversion efficiency is then attenuated because the different Poynting vectors are not collinear and the beams do not overlap. Type I and type II are not equivalent in terms of walk-off angles. For type I, the two fundamental waves have the same polarization $\mathbf{E}^+$ and the same walk-off angle ρ^+, which is different from the harmonic one; thus the coordinate systems that are involved in equations (1.7.3.22) are $(X_1, Y_1, Z) = (X_2, Y_2, Z) = (X^+_\omega, Y^+_\omega, Z)$ and $(X_3, Y_3, Z) = (X^-_{2\omega}, Y^-_{2\omega}, Z)$. For type II, the two fundamental waves have necessarily different walk-off angles ρ^+ and ρ^-, which forbids the nonlinear interaction beyond the plane where the two fundamental beams are completely separated. In this case we have three different coordinate systems: $(X_1, Y_1, Z) = (X^+_\omega, Y^+_\omega, Z)$, $(X_2, Y_2, Z) = (X^-_\omega, Y^-_\omega, Z)$ and $(X_3, Y_3, Z) = (X^-_{2\omega}, Y^-_{2\omega}, Z)$.

The three coordinate systems are linked by the refraction angles ρ of the three waves as explained in Section 1.7.3.2.1. We consider Gaussian transverse profiles: the electric field amplitude is then given by (1.7.3.37). In these conditions, the integration of (1.7.3.22) over (X, Y, Z) by assuming $\tan\rho = \rho$, the non-depletion of the pump and, in the case of phase matching, $\Delta k = 0$ leads to the efficiency $\eta_{SHG}(L)$ given by formula (1.7.3.42) with $\sin c^2(\Delta kL/2) = 1$ and multiplied by the factor $[G(L, w_o, \rho)]/[\cos^2\rho(2\omega)]$ where $\rho(2\omega)$ is the harmonic walk-off angle and $G(L, w_o, \rho)$ is the walk-off attenuation function.

For type I, the walk-off attenuation is given by (Boyd *et al.*, 1965)

$$G_I(t) = (\pi^{1/2}/t)\,\mathrm{erf}(t) - (1/t^2)[1 - \exp(-t^2)]$$

with

$$t = (\rho L/w_o) \qquad (1.7.3.53)$$

and

$$\mathrm{erf}(x) = (2/\pi^{1/2}) \int_0^x \exp(-t^2)\,\mathrm{d}t.$$

For uniaxial crystals, $\rho = \rho^e(2\omega)$ for a $2oe$ interaction and $\rho = \rho^e(\omega)$ for a $2eo$ interaction. For the biaxial class, $\rho = \rho^e(2\omega)$ for a $2oe$ interaction and $\rho = \rho^e(\omega)$ for a $2eo$ interaction in the xz and yz planes, $\rho = \rho^o(\omega)$ for a $2oe$ interaction and $\rho = \rho^o(2\omega)$ for a $2eo$ interaction in the xy plane. For any direction of propagation not contained in the principal planes of a biaxial crystal, the fundamental and harmonic waves have nonzero walk-off angles, respectively $\rho^+(\omega)$ and $\rho^-(2\omega)$. In this case, (1.7.3.53) can be used with $\rho = |\rho^+(\omega) - \rho^-(2\omega)|$.

(*a*) For small t ($t \ll 1$), $G_I(t) \simeq 1$ and $P^{2\omega}(L) \equiv L^2$,

(*b*) For large t ($t \gg 1$), $G_I(t) \simeq (\pi^{1/2}/t)$ and so $P^{2\omega}(L) \equiv L/\rho$ according to (1.7.3.42) with $\Delta k = 0$.

For type II, we have (Mehendale & Gupta, 1988)

$$G_{II}(t) = (2/\pi^{1/2}) \int_{-\infty}^{+\infty} F^2(a, t)\,\mathrm{d}a$$

with

$$F(a, t) = (1/t)\exp(-a^2) \int_0^t \exp[-(a + \tau)^2]\,\mathrm{d}\tau \qquad (1.7.3.54)$$

and

$$a = \frac{r}{w_o} \quad \tau = \frac{\rho u}{w_o} \quad t = \frac{\rho L}{w_o}.$$

r and u are the Cartesian coordinates in the walk-off plane where u is collinear with the three wavevectors, *i.e.* the phase-matching direction.

$\rho = \rho^e(\omega)$ for (oeo) in uniaxial crystals and in the xz and yz planes of biaxial crystals. $\rho = \rho^o(\omega)$ in the xy plane of biaxial crystals for an (eoe) interaction.

For the interactions where $\rho^-(2\omega)$ and $\rho^-(\omega)$ are nonzero, we assume that they are close and contained in the same plane, which is generally the case. Then we classically take ρ to be the maximum value between $|\rho^-(2\omega) - \rho^+(\omega)|$ and $|\rho^-(\omega) - \rho^+(\omega)|$. This approximation concerns the (eoe) configuration of polarization in uniaxial crystals and for biaxial crystals in the xz and yz planes, in the xy plane for (oeo) and out of the principal planes for all the configurations of polarization.

The exact calculation of G, which takes into account the three walk-off angles, $\rho^-(\omega)$, $\rho^+(\omega)$ and $\rho^-(2\omega)$, was performed in the case where these three angles were coplanar (Asaumi, 1992). The exact calculation in the case of $KTiOPO_4$ (KTP) for type-II SHG at 1.064 μm gives the same result for $L/z_R < 1$ as for one angle defined as previously (Fève *et al.*, 1995), which includes the parallel-beam limit $L/z_R <$ 0.3–0.4: $z_R = [k(\omega)w_o^2]/2$ is the Rayleigh length of the fundamental beam inside the crystal.

(*a*) For $t \ll 1$, $G_{II}(t) \simeq 1$, leading to the L^2 dependence of $P^{2\omega}(L)$.

(*b*) For $t \gg 1$, $G_{II}(t) \simeq (t_a^2/t^2)$ with $t_a = [(2)^{1/2} \arctan(2^{1/2})]^{1/2}$, corresponding to a saturation of $P^{2\omega}(L)$ because of the walk-off between the two fundamental beams as shown in Fig. 1.7.3.9.

The saturation length, $L_{\rm sat}$, is defined as $2.3 t_a w_o/\rho$, which corresponds to the length beyond which the SHG conversion efficiency varies less than 1% from its saturation value $BP^{\omega}(0)t_a^2/\rho^2$.

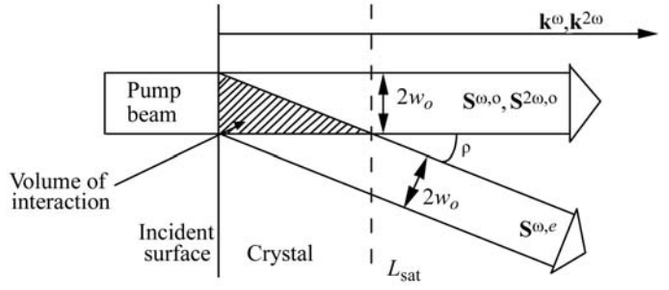

Fig. 1.7.3.9. Beam separation in the particular case of type-II (*oeo*) SHG out of the *xy* plane of a positive uniaxial crystal or in the *xz* and *yz* planes of a positive biaxial crystal. $\mathbf{S}^{\omega,o}$, $\mathbf{S}^{\omega,e}$ and $\mathbf{S}^{2\omega,o}$ are the fundamental and harmonic Poynting vectors; $\mathbf{k}^{\omega}$ and $\mathbf{k}^{2\omega}$ are the associated wavevectors collinear to the CPM direction. w_o is the fundamental beam radius and ρ is the walk-off angle. $L_{\rm sat}$ is the saturation length.

The complete splitting of the two fundamental beams does not occur for type I, making it more suitable than type II for strong focusing. The fundamental beam splitting for type II also leads to a saturation of the acceptance bandwidths $\delta\xi$ ($\xi = \theta, \varphi, T, \lambda$), which is not the case for type I (Fève *et al.*, 1995). The walk-off angles also modify the transversal distribution of the generated harmonic beam (Boyd *et al.*, 1965; Mehendale & Gupta, 1988): the profile is larger than that of the fundamental beam for type I, contrary to type II.

The walk-off can be compensated by the use of two crystals placed one behind the other, with the same length and cut in the same CPM direction (Akhmanov *et al.*, 1975): the arrangement of the second crystal is obtained from that of the first one by a π rotation around the direction of propagation or around the direction orthogonal to the direction of propagation and contained in the walk-off plane as shown in Fig. 1.7.3.10 for the particular case of type II (*oeo*) in a positive uniaxial crystal out of the *xy* plane.

The twin-crystal device is potentially valid for both types I and II. The relative sign of the effective coefficients of the twin crystals depends on the configuration of polarization, on the relative arrangement of the two crystals and on the crystal class. The interference between the waves generated in the two crystals is destructive and so cancels the SHG conversion efficiency if the two effective coefficients have opposite signs: it is always the case for certain crystal classes and configurations of polarization (Moore & Koch, 1996).

Such a tandem crystal was used, for example, with $KTiOPO_4$ (KTP) for type-II SHG at $\lambda_{\omega} = 1.3$ µm ($\rho = 2.47^{\circ}$) and $\lambda_{\omega} = 2.532$ µm ($\rho = 2.51^{\circ}$): the conversion efficiency was about 3.3 times the efficiency in a single crystal of length $2L$, where L is the length of each crystal of the twin device (Zondy *et al.*, 1994). The two crystals have to be antireflection coated or contacted in order to avoid Fresnel reflection losses.

Non-collinear phase matching is another method allowing a reduction of the walk-off, but only in the case of type II (Dou *et al.*, 1992). Fig. 1.7.3.11 illustrates the particular case of (*oeo*) type-II SHG for a propagation out of the *xy* plane of a uniaxial crystal, or in the *xz* or *yz* plane of a biaxial crystal.

In the configuration of special non-collinear phase matching, the angle between the fundamental beams inside the crystal is chosen to be equal to the walk-off angle ρ. Then the associated Poynting vectors $\mathbf{S}^{\omega,o}$ and $\mathbf{S}^{\omega,e}$ are along the same direction, while that of the generated wave deviates from them only by approximately $\rho/2$. The calculation performed in the case of special non-collinear phase matching indicates that it is possible to increase type-II SHG conversion efficiency by 17% for near-field undepleted Gaussian beams (Dou *et al.*, 1992). Another advantage of such geometry is to turn type II into a pseudo type I with respect to the walk-off,

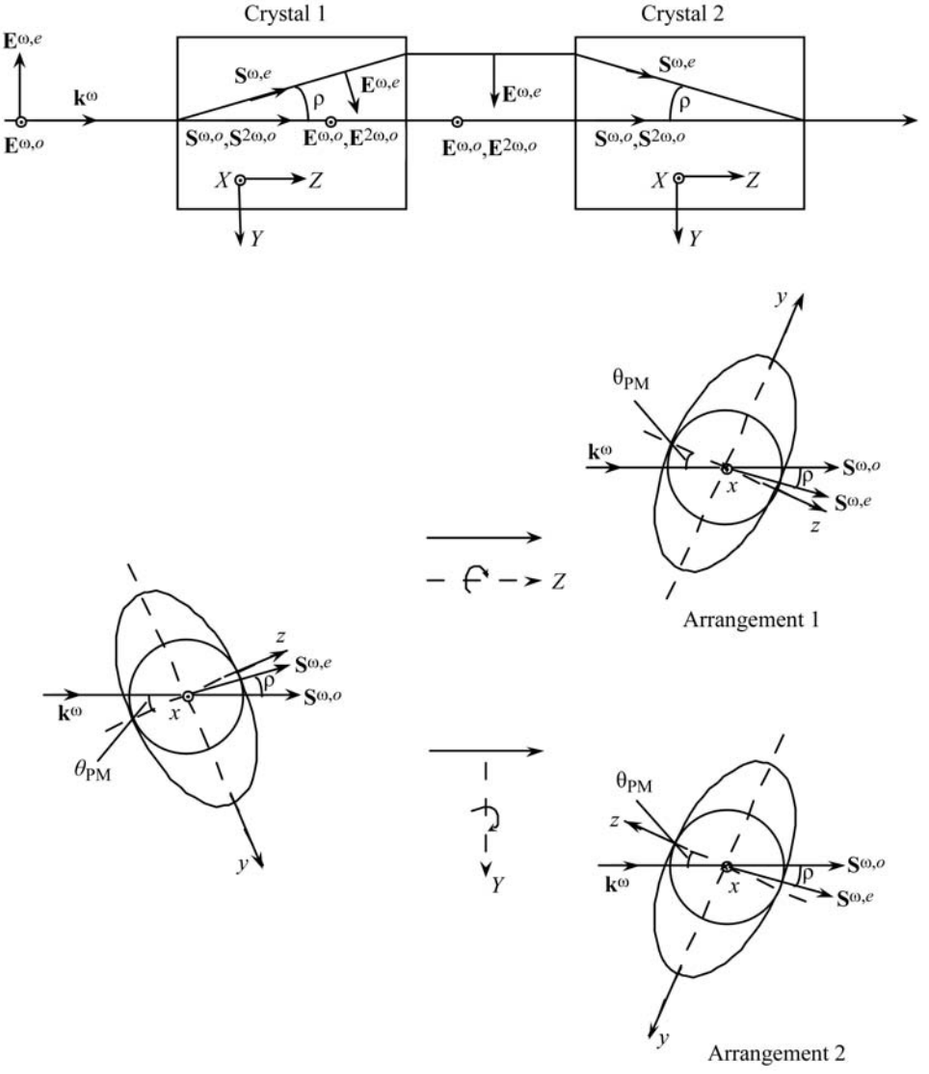

Fig. 1.7.3.10. Twin-crystal device allowing walk-off compensation for a direction of propagation $\theta_{\rm PM}$ in the *yz* plane of a positive uniaxial crystal. (X, Y, Z) is the wave frame and (x, y, z) is the optical frame. The index surface is given in the *yz* plane. $\mathbf{k}^{\omega}$ is the incident fundamental wavevector. The refracted wavevectors $\mathbf{k}^{\omega,o}$, $\mathbf{k}^{\omega,e}$ and $\mathbf{k}^{2\omega,o}$ are collinear and along $\mathbf{k}^{\omega}$. $\mathbf{S}^{\omega,o}$, $\mathbf{S}^{\omega,e}$ and $\mathbf{S}^{2\omega,o}$ are the Poynting vectors of the fundamental and harmonic waves. $\mathbf{E}^{\omega,o}$, $\mathbf{E}^{\omega,e}$ and $\mathbf{E}^{2\omega,o}$ are the electric field vectors. ρ is the walk-off angle.

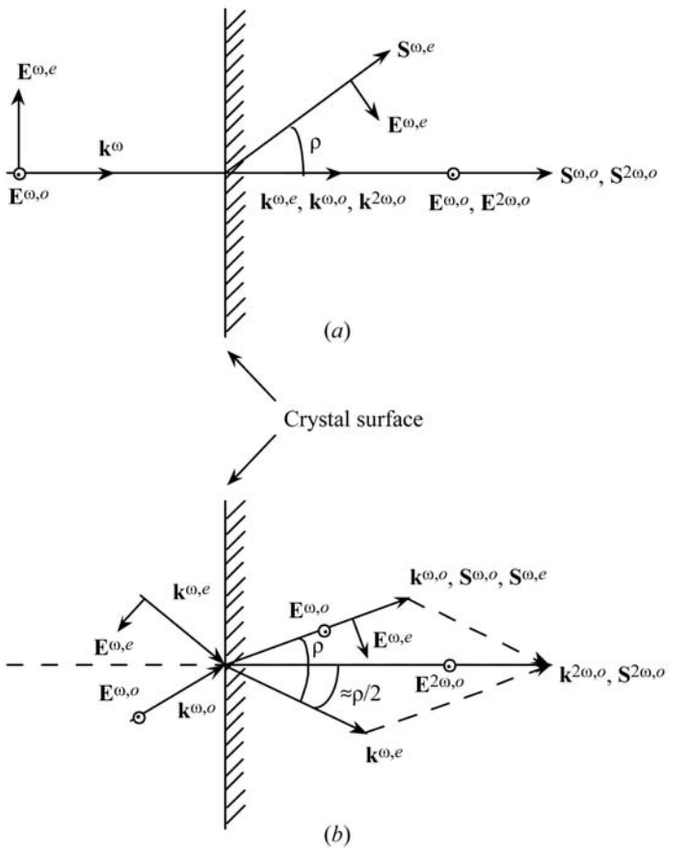

Fig. 1.7.3.11. Comparison between (*a*) collinear and (*b*) special non-collinear phase matching for (*oeo*) type-II SHG. $\mathbf{k}^{\omega,o}$, $\mathbf{k}^{\omega,e}$ and $\mathbf{k}^{2\omega,o}$ are the wavevectors, $\mathbf{S}^{\omega,o}$, $\mathbf{S}^{\omega,e}$ and $\mathbf{S}^{2\omega,o}$ are the Poynting vectors of the fundamental and harmonic waves, and $\mathbf{E}^{\omega,o}$, $\mathbf{E}^{\omega,e}$ and $\mathbf{E}^{2\omega,o}$ are the electric field vectors; ρ is the walk-off angle in the collinear case and the angle between $\mathbf{k}^{\omega,o}$ and $\mathbf{k}^{\omega,e}$ inside the crystal for the non-collinear interaction.

because the saturation phenomenon of type-II CPM is avoided.

(iv) *Effect of temporal walk-off.*

Even if the SHG is phase matched, the fundamental and harmonic group velocities, $v_g(\omega) = \partial\omega/\partial k$, are generally mismatched. This has no effect with continuous wave (c.w.) lasers. For pulsed beams, the temporal separation of the different beams during the propagation can lead to a decrease of the temporal overlap of the pulses. Indeed, this walk-off in the time domain affects the conversion efficiency when the pulse separations are close to the pulse durations. Then after a certain distance, L_τ, the pulses are completely separated, which entails a saturation of the conversion efficiency, for both types I and II (Tomov *et al.*, 1982). Three group velocities must be considered for type II. Type I is simpler, because the two fundamental waves have the same velocity, so $L_\tau = \tau/[v_g^{-1}(\omega) - v_g^{-1}(2\omega)]$, which defines the optimum crystal length, where τ is the pulse duration. For type-I SHG of 532 nm in KH_2PO_4 (KDP), $v_g(266\text{ nm}) = 1.84 \times 10^8\text{ m s}^{-1}$ and $v_g(532\text{ nm}) = 1.94 \times 10^8\text{ m s}^{-1}$, so $L_\tau = 3.5$ mm for 1 ps. For the usual nonlinear crystals, the temporal walk-off must be taken into account for pico- and femtosecond pulses.

1.7.3.3.2.2. *Non-resonant SHG with undepleted pump and transverse and longitudinal Gaussian beams*

We now consider the general situation where the crystal length can be larger than the Rayleigh length.

The Gaussian electric field amplitudes of the two eigen electric field vectors inside the nonlinear crystal are given by

$$E^{\pm}(X, Y, Z) = E_o^{\pm}\frac{w_o}{w(Z)}\exp\left[-\frac{(X+\rho^+Z)^2 + (Y+\rho^-Z)^2}{w^2(Z)}\right] \times \exp\left(i\left\{k^{\pm}Z - \arctan(Z/z_R) + \frac{k^{\pm}\left[(X+\rho^+Z)^2 + (Y+\rho^-Z)^2\right]}{2Z\left[1+(z_R^2/Z^2)\right]}\right\}\right) \quad (1.7.3.55)$$

with $\rho^- = 0$ for E^+ and $\rho^+ = 0$ for E^-.

(X, Y, Z) is the wave frame defined in Fig. 1.7.3.1. $E_o^{\pm}$ is the scalar complex amplitude at $(X, Y, Z) = (0, 0, 0)$ in the vibration planes $\Pi^{\pm}$.

We consider the refracted waves E^+ and E^- to have the same longitudinal profile inside the crystal. Then the $(1/e^2)$ beam radius is given by $w(Z)^2 = w_o^2[1 + (Z^2/z_R^2)]$, where w_o is the minimum beam radius located at $Z = 0$ and $z_R = kw_o^2/2$, with $k = (k^+ + k^-)/2$; z_R is the Rayleigh length, the length over which the beam radius remains essentially collimated; $k^{\pm}$ are the wavevectors at the wavelength λ in the direction of propagation Z. The far-field half divergence angle is $\Delta\alpha = 2/kw_o$.

The coordinate systems of (1.7.3.22) are identical to those of the parallel-beam limit defined in (iii).

In these conditions and by assuming the undepleted pump approximation, the integration of (1.7.3.22) over (X, Y, Z) leads to the following expression of the power conversion efficiency (Zondy, 1991):

$$\eta_{\text{SHG}}(L) = \frac{P^{2\omega}(L)}{P^{\omega}(0)} = CLP^{\omega}(0)\frac{h(L, w_o, \rho, f, \Delta k)}{\cos^2\rho_{2\omega}}$$

with

$$C = 5.95 \times 10^{-2}\frac{2N-1}{N}\frac{d_{\text{eff}}^2}{\lambda_\omega^3}\frac{n_1^\omega + n_2^\omega}{2}\frac{T_3^{2\omega}T_1^\omega T_2^\omega}{n_3^{2\omega}n_1^\omega n_2^\omega} \quad (\text{W}^{-1}\text{ m}^{-1}) \quad (1.7.3.56)$$

in the same units as equation (1.7.3.42).

For type I, $n_1^\omega = n_2^\omega$, $T_1^\omega = T_2^\omega$, and for type II $n_1^\omega \neq n_2^\omega$, $T_1^\omega \neq T_2^\omega$.

The attenuation coefficient is written

$$h(L, w_o, \rho, f, \Delta k) = [2z_R(\pi)^{1/2}/L]\int_{-\infty}^{+\infty}|H(a)|^2\exp(-4a^2)\,\text{d}a$$

with

$$H(a) = \frac{1}{(2\pi)^{1/2}}\int_{-fL/z_R}^{L(1-f)/z_R}\frac{\text{d}\tau}{1+i\tau}\exp\left[-\gamma^2\left(\tau + \frac{fL}{z_R}\right)^2 - i\sigma\tau\right]$$

$$\text{for type I: } \gamma = 0 \text{ and } \sigma = \Delta k z_R + 4\frac{\rho z_R}{w_o}a$$

$$\text{for type II: } \gamma = \frac{\rho z_R}{w_o(2)^{1/2}} \text{ and } \sigma = \Delta k z_R + 2\frac{\rho z_R}{w_o}a, \quad (1.7.3.57)$$

where f gives the position of the beam waist inside the crystal: $f = 0$ at the entrance and $f = 1$ at the exit surface. The definition and approximations relative to ρ are the same as those discussed for the parallel-beam limit. Δk is the mismatch parameter, which takes into account first a possible shift of the pump beam direction from the collinear phase-matching direction and secondly the distribution of mismatch, including collinear and non-collinear interactions, due to the divergence of the beam, even if the beam axis is phase-matched.